

# Fuzzy Inference System for Modeling the Contribution of the Sweep Mechanism in the Coagulation Process for Water Treatment



This work is licensed under a Creative Commons Attribution 4.0 International License

D. G. Marques,\* G. Gomes, J. V. L. Cardoso, L. H. F. Aiello,  
S. R. M. M. Roveda, J. A. F. Roveda, and V. Campos

Institute of Science and Technology,  
São Paulo State University (UNESP),  
Sorocaba, SP, Brazil

doi: <https://doi.org/10.15255/CABEQ.2025.2415>

Original scientific paper  
Received: February 20, 2025  
Accepted: May 28, 2025

Coagulation is a critical step in water treatment, with polyaluminum chloride being a commonly used coagulant. Its main mechanisms are charge neutralization and sweep coagulation. Minimizing sweep coagulation, when appropriate, can reduce chemical use and improve sludge management. A Fuzzy Inference System (FIS) is an effective tool for handling uncertainties and is often used for simplified process modeling. In this study, a FIS was developed to estimate the contribution of the sweep mechanism using zeta potential, insoluble aluminum content, and turbidity removal as inputs. The model used three input variables and nine rules, aiming for low computational demand. The highest estimated sweep contribution occurred at pH slightly basic and Al(s) concentration  $> 2 \text{ mg L}^{-1}$  in a natural low-turbidity water sample. The FIS enabled the integration of frequent measured variables into a single numerical output estimation linked to coagulation mechanisms, supporting decision-making and enabling opportunities for automation and cost reduction.

## Keywords

water treatment, modeling, fuzzy logic, sweep mechanism, polyaluminum chloride

## Introduction

Several physical and chemical processes are applied in water treatment for public supply purposes, aiming to remove impurities and ensure safe water quality for consumption. In a conventional water treatment plant (WTP), the main processes include coagulation-flocculation, sedimentation, filtration, and disinfection<sup>1</sup>. Disinfection is the primary operation related to biosafety, preventing waterborne illnesses through the inactivation of microorganisms and viruses<sup>2</sup>. Coagulation-flocculation, in turn, is associated with the aggregation of particles into flocs, which are subsequently removed through solid-liquid separation processes such as sedimentation and filtration<sup>3</sup>. Additional processes may also be included, depending on the specific characteristics of the water. These may involve adsorption, used for the removal of natural organic matter<sup>4</sup>, metals, and microbes<sup>5</sup>; membrane separation, capable of removing bacteria, viruses, low molecular weight organic compounds, and ionic species<sup>6</sup>; and advanced oxidation processes (AOPs), which have been reported to target emerging pollutants such as microplastics<sup>7</sup>, recalcitrant chemicals and endocrine disrupting compounds<sup>8</sup>.

Coagulation is a key process for drinking-water production, and is described as the step in which the destabilization of organic and inorganic particles in water occurs, facilitating their aggregation during the subsequent flocculation stage. The formation of dense, large, and heavy flocs is essential for effective separation in subsequent steps, such as sedimentation, flotation, or filtration<sup>9,10</sup>, underscoring the importance of a successful coagulation-flocculation process. Common chemical coagulants include iron and aluminum salts, such as ferrous sulfate, aluminum sulfate, and polyaluminum chloride (PACl)<sup>11</sup>. PACl is noted for its efficiency and competitive price, which has led to its widespread use over other market options<sup>12</sup>.

The primary mechanisms involved in the coagulation process with PACl are charge neutralization and the sweep mechanism<sup>13</sup>. The charge neutralization mechanism reduces the electrostatic repulsion between colloidal particles, enabling their collision and aggregation. In contrast, the sweep mechanism relies on the extensive formation of insoluble hydroxides, such as  $\text{Al}(\text{OH})_3(\text{s})$ , under high PACl doses and specific pH ranges, which physically enmesh and remove colloidal particles from the water<sup>14</sup>. The sweep mechanism, however, is associated with higher reagent costs due to the increased coagulant

\*Corresponding author: [diego.marques@unesp.br](mailto:diego.marques@unesp.br)

dose and greater demand for alkalizing agents for pH correction, compared to the charge neutralization mechanism<sup>15</sup>. Additionally, zeta potential measurement is used for charge control in water, and its values significantly influence the success of charge neutralization coagulation. On the other hand, the sweep mechanism is described as less dependent on zeta potential values<sup>16</sup>.

Determining the required coagulant dose is a highly non-linear process, as it depends on various factors and involves complex chemical interactions<sup>17</sup>. To better understand this process, coagulation mechanism diagrams have been developed, illustrating a wide range of coagulant doses and pH levels, as well as presenting lines of insoluble formation and suggesting zones where different mechanisms typically are observed, such as charge neutralization, sweep mechanism, restabilization, and mixed mechanisms<sup>18</sup>. Simpler coagulation diagrams are also used in experimental results, relating coagulant doses to pH and residual turbidity in treated water samples<sup>19,20</sup>. However, these conventional diagrams tend to better depict turbidity reduction zones without detailing the contributions of individual mechanisms. Given that each mechanism has distinct characteristics, advantages, and applicability for specific scenarios, a more nuanced understanding of these contributions could lead to more informed decision-making regarding treatment efficiency and cost reduction.

In this context, FIS have emerged as a promising and attractive alternative for managing a wide range of variables with inherent uncertainty. FIS combine fuzzy logic with expert systems, allowing for the use of subjective, vague, ambiguous, or incomplete data<sup>21</sup>. This combination serves as a powerful tool for interpreting and analyzing complex systems based on approximate relationships<sup>22</sup>, such as the non-linear coagulation process<sup>23</sup>. One of the advantages of this approach is the incorporation of expert knowledge into the modeling process, which enhances the precision and reliability of the results<sup>24</sup>. FIS are based on fuzzy rules and adopt an “if... then” structure, where the efficacy of the models depends on the accuracy of the parameters estimated in the model<sup>16</sup>. The main types of FIS are the Mamdani, Sugeno, and Tsukamoto systems<sup>17</sup>. The Mamdani-type FIS, in addition to its known ability to handle complex processes that are difficult to model mathematically, is also recognized for being tractable and widely used in automatic control systems<sup>25</sup>.

In the field of water treatment for public supply, several studies have developed and applied fuzzy logic models to determine the optimal coagulant dose and control the coagulation process<sup>17,22,26,27</sup>.

These studies emphasize the advantages of mathematical modeling over experimental approaches in coagulation studies, noting that experimental methods are often associated with higher costs and lengthy routines. Bressane *et al.*<sup>27</sup> also argue that jar testing is ineffective for real-time adjustments, while Arpitha and Pani<sup>28</sup> cite that automatic control is essential to aim process safety and quality enhancement, highlighting the benefits of data-driven technologies.

In the previously mentioned studies with FIS in water treatment coagulation, the number of input variables ranged from two to six, primarily related to raw water parameters, data from real treatment plants, or jar testing, and the number of fuzzy rules varied significantly. A common aspect among the studies was the integration of FIS with machine-learning approaches such as Adaptive Neuro-Fuzzy Inference System (ANFIS) and other data-driven models. While such combinations may improve model robustness and accuracy, their utilization often requires substantial computational resources<sup>26</sup>. Another limitation noted by Salleh *et al.*<sup>29</sup>, is that ANFIS implementations are normally restricted to applications that offer large datasets for the training. Given that coagulation dosing in WTPs is often based on empirical knowledge and operators' subjective judgment<sup>30</sup>, the use of highly complex models may be disproportionate to the practical reality. In this context, a simplified model may offer a viable intermediate alternative by balancing modeling complexity, computational costs, while remaining suitable for real-world applications and facilitating the handling of the coagulation process.

This study aimed to develop a Mamdani-type FIS using zeta potential, insoluble aluminum content, and residual turbidity as input variables to estimate the predominance of the sweep coagulation mechanism. The model was designed to be computationally efficient, relying on three input variables and nine fuzzy rules. The work includes experimental jar tests, modeling structure, membership function definitions and their limits, the logical premises adopted in rule construction, model application, and analysis of the obtained results.

## Material and methods

The raw water sample used in this research was collected from the Cachoeira do França reservoir in São Paulo, a preserved water source that supplies the Metropolitan Region of São Paulo<sup>31</sup>. The same batch of water was used throughout the entire analysis, minimizing temporal variations in raw water quality and ensuring its homogeneity. The sample had a turbidity level below 10 NTU (Nephelometric

Turbidity Unit), indicating low-turbidity water, as defined by Cruz *et al.*<sup>32</sup> The experiments were conducted using a PoliControl Floc Control jar test apparatus, which had six jars and a maximum rotation speed of 300 rpm. A total of 30 test runs were used to construct the coagulation diagram.

The coagulant used in the study was PAC Floc 120 HT from Bauminas®, with an Al<sub>2</sub>O<sub>3</sub> content ranging between 9 % and 11 %. The total aluminum content was measured using the Hach 8012 method, yielding a value of 4.92 %. The Al dose varied from 0.88 to 3.52 mg L<sup>-1</sup>, while the pH ranged from 5 to 8.3 adapting the diagrams developed by Bartiko and Julio<sup>20</sup>. The pH value was estimated in preliminary bench-scale studies, and the corresponding NaOH concentration for each point was added to the jars prior to the start of the experiment. For the physicochemical analysis of both raw and treated water, the following instruments were used: a Hach TU5200 Turbidimeter, a Thermo Scientific Orion Dual Star pH meter, a Malvern Zetasizer Nano Series zeta potential meter, and a Mettler Toledo UV5 spectrophotometer.

The proposed FIS utilized zeta potential, the concentration of insoluble Al in the form of Al(OH)<sub>3</sub>(s) (referred to as Al(s) concentration), and turbidity removal percentage as input variables. Although pH is a known variable influencing coagulation mechanisms, its effect was considered to be implicitly represented through the zeta potential and Al(s) concentration inputs. The system was implemented using MATLAB® software using the Fuzzy Logic Designer tool. Membership functions for the input variables were either triangular or trapezoidal, depending on the characteristics of each linguistic variable. Their limits were defined based on trends observed in experimental data and information from the literature.

The output “sweep contribution” is represented by a triangular membership function with five equidistant fuzzy sets: very low, low, medium, high, and very high. These fuzzy sets, defined based on linguistic terms, aim to simplify the uncertainty of the results and enable the aggregation of similar behaviors into a single output. The number of fuzzy sets for the linguistic variable in the output was chosen based on the number of results that allow for association without overlapping the “if...then” rules. Defuzzification was carried out using the centroid method, and the numeric output ranged from 0 to 10, aiming to facilitate visualization. The rule base was constructed from six logical premises derived from coagulation process understanding, assuming equal weighting for Al(s) concentration and turbidity removal, which resulted in nine rules encompassing all possible scenarios.

## Results and discussion

The results are divided into three sections: (a) results of the jar test assays, (b) development of the fuzzy inference system, and (c) application of data to the system.

### Jar test assays

The jar test assays revealed relationships between the variables, helping define the limits for the membership functions. Measurements were taken for pH, residual turbidity after sedimentation, and zeta potential. The physicochemical characteristics of the raw water and the hydraulic variables employed during the jar test assays are presented in Table 1.

Fig. 1 displays a contour diagram showing the distribution of residual turbidity values by Al dose, referred to as Al<sub>total</sub> concentration, and pH. The dark blue zone indicates better turbidity reduction, with final values approaching 0 NTU for Al doses above 2 mg L<sup>-1</sup> and pH ranging from approximately 6.8 to 8.5.

Further interpreting of a coagulation diagram focused on assessing the quantity of hydrolyzed precipitates that were formed for each point, as this is the main step of the sweep mechanism. Sweep coagulation is associated with higher turbidity removal and is often used in lower-quality water or more complex treatments<sup>15</sup>. For cleaner water sources, minimizing the sweep mechanism is related to savings in reagents and reduced sludge production. According to a diagram of coagulation mechanisms described by Benson<sup>18</sup>, the data points within this pH and Al<sub>total</sub> concentration span various mechanism ranges, from charge neutralization to zones of restabilization, neutralization with Al(OH)<sub>3</sub>(s) at zero zeta potential, coagulation with mixed mechanisms, and sweep flocculation. The presence of data in zones of uncertainty regarding the dominant mechanism supports the use of a FIS.

Table 1 – Physicochemical characteristics of the raw water and hydraulic variables during jar test assays

Parameter	Value
Turbidity	5.89±0.84 NTU
pH	6.80±0.05
Zeta potential	-16.4±1.1 mV
Rapid mixing time	10 s
Rapid mixing velocity gradient	600 s <sup>-1</sup>
Slow mixing time	15 min
Slow mixing velocity gradient	35 s <sup>-1</sup>
Sedimentation time	7 min

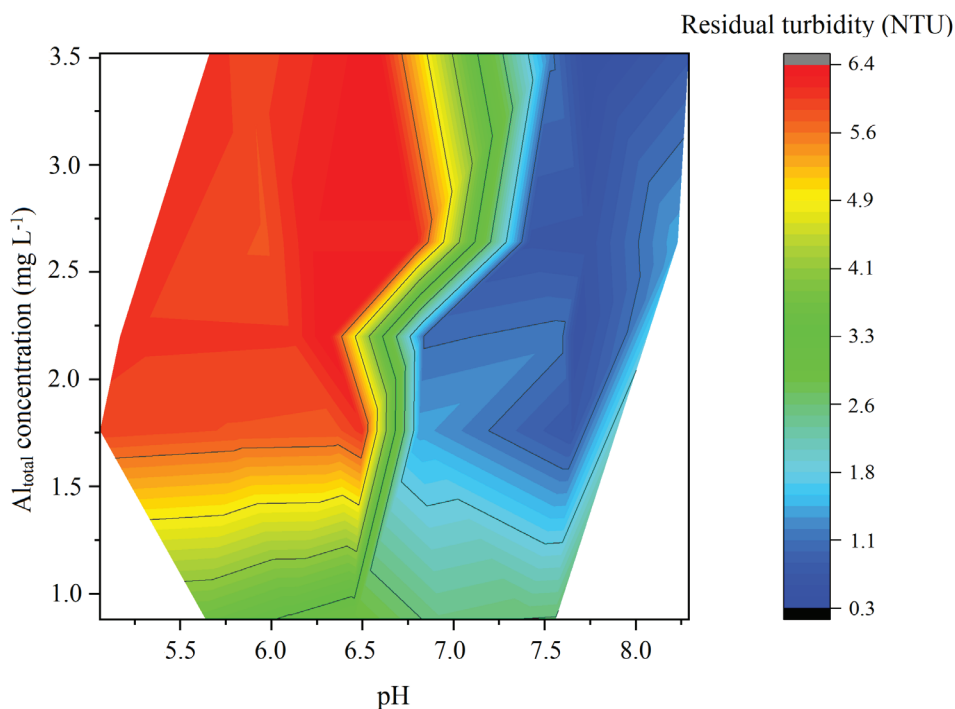


Fig. 1 – Contour diagram of residual turbidity in NTU in a pH and total Al concentration coagulation diagram

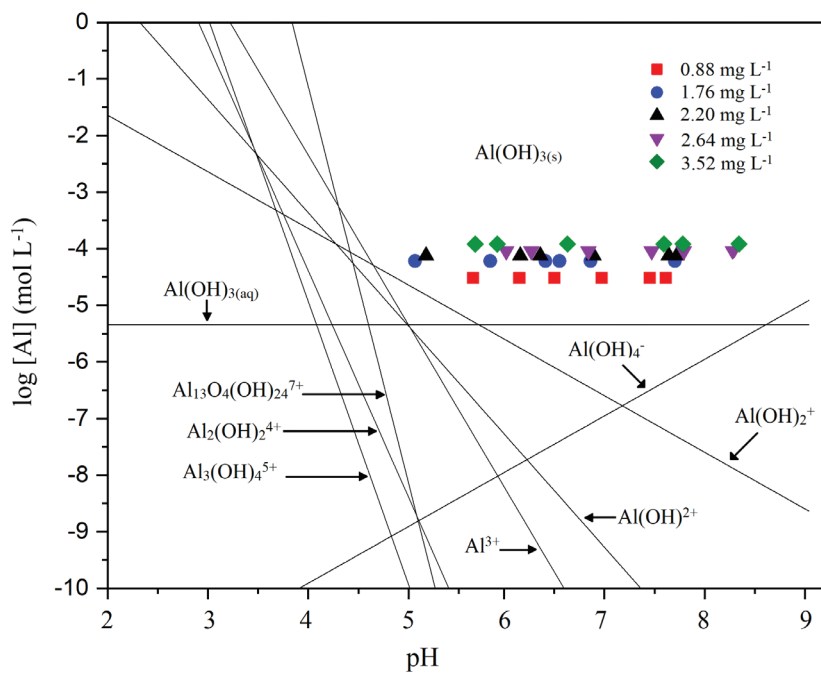


Fig. 2 – Sample distribution on an aluminum solubility diagram

Fig. 2 illustrates the distribution of the samples on an Al solubility diagram by pH, using data from Xiao *et al.*<sup>33</sup> It shows that all samples were above the  $\text{Al(OH)}_3(\text{s})$  solubility curve, indicating the formation of insoluble Al.

Calculations were performed to determine the percentage of Al(s) for the different doses, and the ratio of Al(s) to  $\text{Al}_{\text{total}}$  is shown in Fig. 3. The results

indicate that only at pH levels below 6 and for doses from 0.88 to 2.20  $\text{mg L}^{-1}$  of Al does the fraction of insoluble aluminum comprise less than 75 % of the total aluminum.

In the zone where coagulation occurs mainly by charge neutralization, the predominance of soluble hydrolyzed species is observed, and, therefore, it is below the  $\text{Al(OH)}_3(\text{s})$  curve. Conversely, the

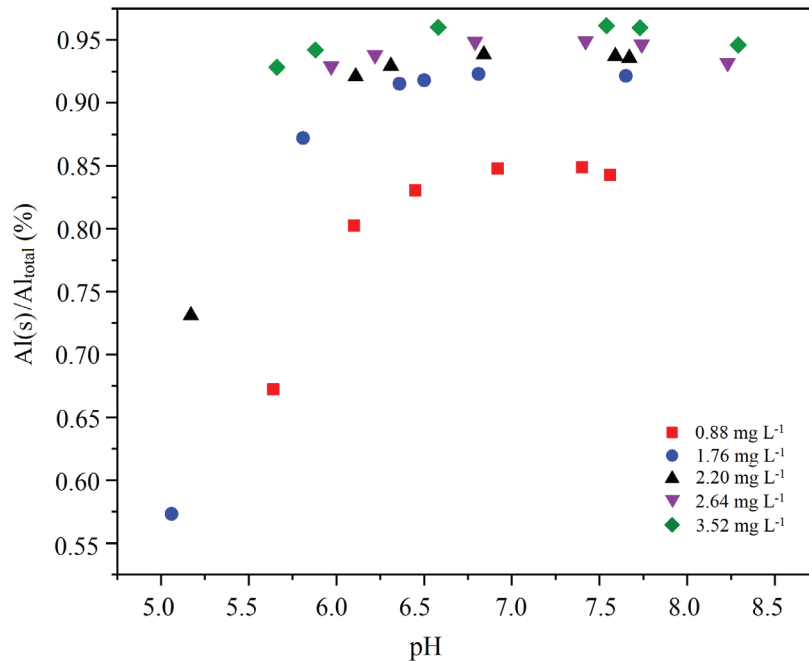


Fig. 3 – Percentage of  $Al(s)$  relative to initial  $Al$  dose

points representing  $Al$  doses and  $pH$  used to construct the work diagram are expected, according to the mechanisms diagram proposed by Benson<sup>18</sup>, to be primarily located in the zones of re-stabilization, charge neutralization with  $Al(OH)_3(s)$ , mixed mechanisms, and sweep mechanisms. The re-stabilization zone is associated with the absence of coagulation, while charge neutralization with  $Al(OH)_3(s)$  and mixed mechanisms involve a combination of both main mechanisms, in zones of uncertainty of main contributions. The proposed FIS aimed to numerically estimate the predominance of the sweep mechanism over the charge neutralization mechanism based on the evaluated parameters.

### Defining limits for membership functions

The input variables include zeta potential,  $Al(s)$  concentration, and turbidity removal percentage. To define the limits for the membership functions, data from the literature were adapted and interpreted alongside the experimental data.

For zeta potential, Fig. 4 shows the distribution of residual turbidity according to zeta potential. For values ranging from  $-15$  mV to approximately  $5$  mV, residual turbidity varied among samples, ranging from nearly  $0$  NTU to as high as  $4$  NTU. This variation suggests that zeta potential and neutralization mechanisms do not function in isolation. In contrast, unsatisfactory coagulation was observed at zeta potential values above  $+10$  mV, where residual turbidity was close to that of the raw water ( $5.89$  NTU). Accordingly, this observation was taken into account when establishing the limits of the membership function.

The neutral zeta potential, or isoelectric point, is generally considered optimal for coagulation-flocculation through the charge neutralization mechanism<sup>34</sup>. Additionally, while Sun *et al.*<sup>35</sup> suggest a broad range of zeta potential from  $-10$  mV to  $+10$  mV for effective coagulation, several authors report narrower ranges. For instance, Ghernaout *et al.*<sup>16</sup>, Sharp *et al.*<sup>36</sup>, and Mroczko and Zimoch<sup>37</sup> observed effective coagulation within the range of  $-10$  mV to  $+5$  mV, while Saritha *et al.*<sup>38</sup> proposed a range of  $-8$  mV to  $+5$  mV, indicating that positive values should remain closer to the isoelectric point compared to the negative ones to avoid disturbing the coagulation process. Consequently, the negative limit for zeta potential is set at values below  $-10$  mV, while the positive limit is set above  $+7$  mV, marking zones where zeta potential may not support, and could even hinder coagulation. The membership function for the zeta potential variable, reflecting these ranges, is shown in Fig. 5.

Regarding  $Al(s)$  concentration, studies have identified two distinct ranges of aluminum coagulant doses: one within a lower concentration that provides satisfactory coagulation and another with a higher concentration that achieves greater coagulation and higher turbidity reduction. Duan and Gregory<sup>39</sup>, for instance, observed two effective coagulation ranges at  $pH$  7: one at a lower concentration of  $15$   $\mu M$   $Al$  ( $0.41$   $mg$   $L^{-1}$ ) and another at a concentration above  $60$   $\mu M$  ( $1.62$   $mg$   $L^{-1}$ ). Concentrations between these two points resulted in low turbidity reduction, likely due to re-stabilization. These two levels were referenced as “medium” and “high” for the membership function modeling. Table 2 pres-

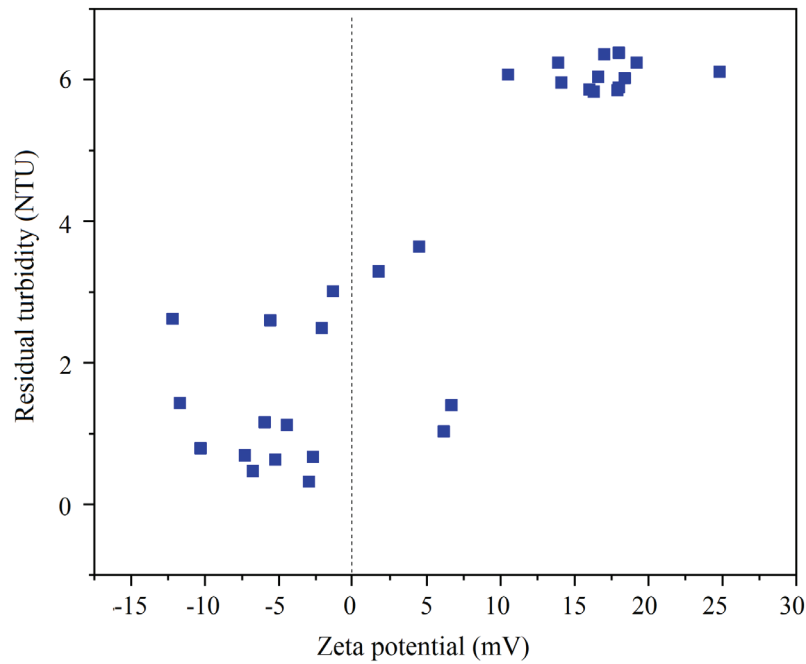


Fig. 4 – Residual turbidity (NTU) in relation to the zeta potential (mV) of the samples

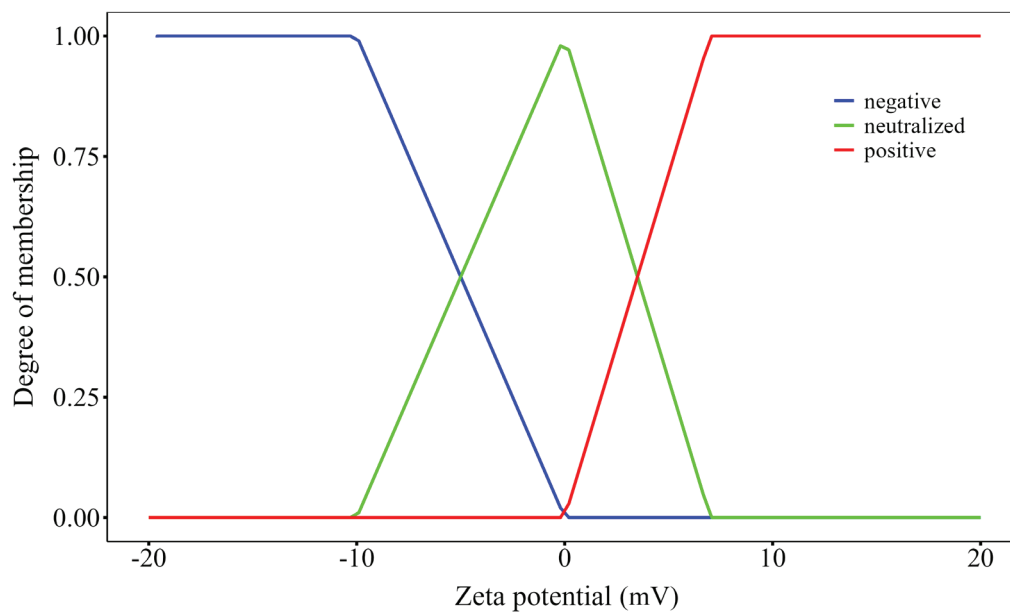


Fig. 5 – Membership function for the zeta potential variable

Table 2 –  $Al_{total}$  concentration in “medium” and “high” levels applied in coagulation assays and their  $Al(s)$  concentrations

Source	$Al_{total}$ concentration ( $mg L^{-1}$ )		pH	$Al(s)$ concentration ( $mg L^{-1}$ )	
	Medium	High		Medium	High
Cruz <i>et al.</i> <sup>32</sup>	0.45	1.36	7.0	0.31	1.22
Duan and Gregory <sup>39</sup>	0.41	1.62	7.0	0.27	1.48
Lin and Ika <sup>40</sup>	0.81	2.43	7.5	0.67	2.29
Yan <i>et al.</i> <sup>41</sup>	0.54	2.16	7.0	0.41	2.02
Trinh and Kang <sup>42</sup>	1.35	3.51	7.5	1.21	3.37
He and Nan <sup>43</sup>	1.00	2.20	7.8	0.85	2.05
Ng <i>et al.</i> <sup>44</sup>	2.16	4.12	6.0	1.97	3.93

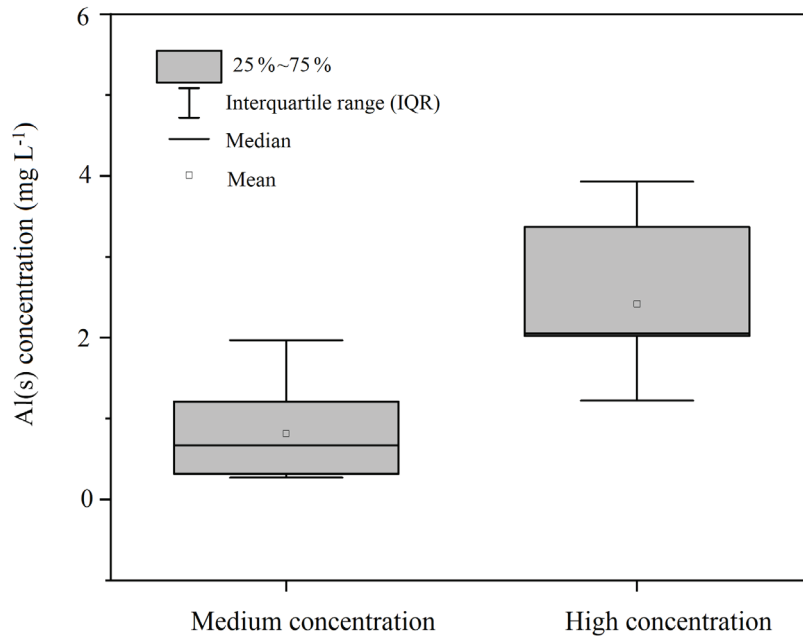


Fig. 6 – Boxplot of  $Al(s)$  concentration data applied in coagulation assays, presented in “medium” and “high” levels

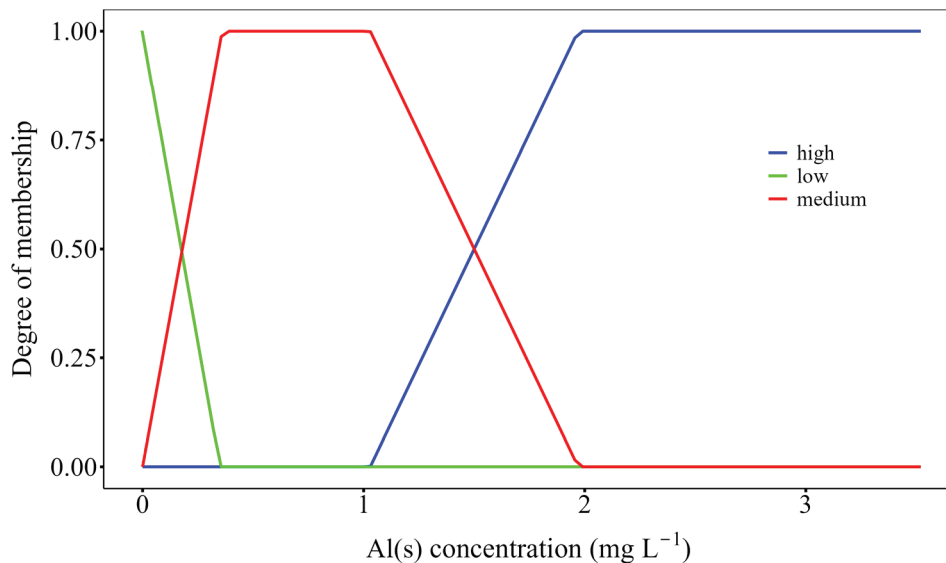


Fig. 7 – Membership function of the  $Al(s)$  concentration variable

ents the  $Al$  doses,  $Al(s)$  concentration, and pH of coagulation, while Fig. 6 shows the boxplot of  $Al(s)$  concentrations obtained.

The linguistic values for the membership function for  $Al(s)$  concentration were divided into “low,” “medium,” and “high” levels, with a domain ranging from 0 to  $3.52 \text{ mg L}^{-1}$ , the maximum dose used in the jar test experiment depicted in Fig. 1. As shown in Fig. 6, the upper whisker limit of the “medium”  $Al(s)$  concentration level nearly overlaps with the lower whisker of the “high” level, indicat-

ing a possible uncertainty point between these linguistic variables. Similarly, uncertainty for the “low” level was defined from  $0 \text{ mg L}^{-1}$  to the minimum value of the “medium”  $Al(s)$  concentration level. Singala *et al.*<sup>45</sup> reinforce that the ability of a single value to be associated with multiple aspects within a membership function is a key feature of the fuzzification and defuzzification processes, enabling linguistic variables to interact with numerical values. The resulting membership function is shown in Fig. 7, with the uncertainty ranging from 0 to 0.36 for the ‘low’ value, and from 1.03 to 1.96 for

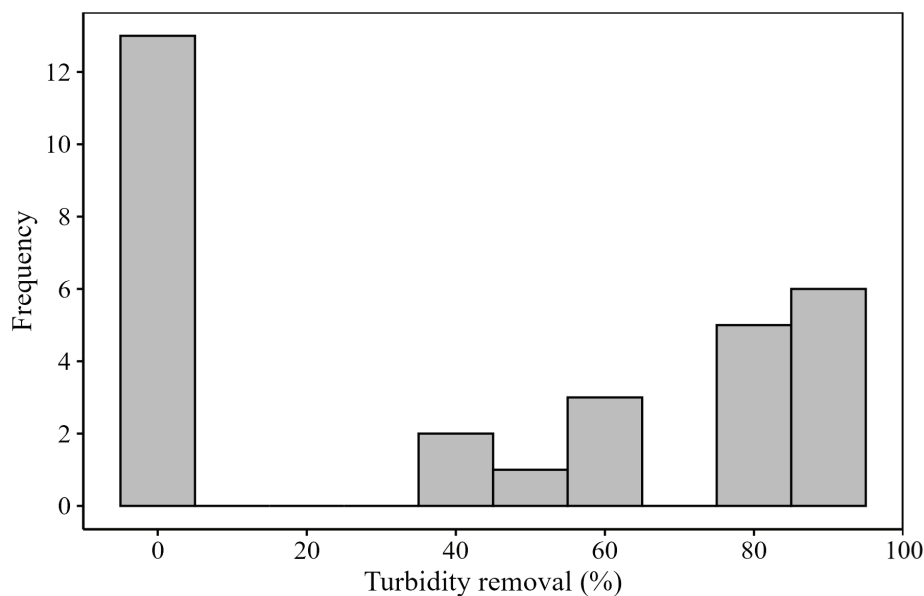


Fig. 8 – Histogram of turbidity removal percentages

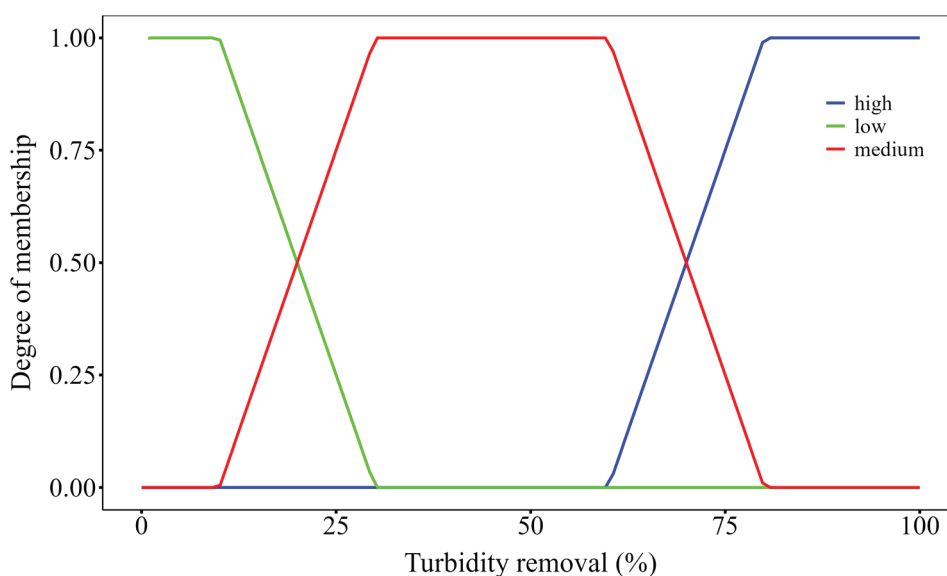


Fig. 9 – Membership function for the turbidity removal variable

the ‘medium’ value, these limits approximate the pattern of overlapping whiskers observed in Fig. 6.

For turbidity removal, the data clustered into three well-defined groups: (1) samples where coagulation did not occur, with removal less than 10 %; (2) samples with intermediate removal ranging from 30 % to 60 %; and (3) samples with removal exceeding 80 %. This allowed the membership function to be adjusted according to the observed behavior, with uncertainty accounted for in the spaces between these zones. The histogram of turbidity removal percentages is shown in Fig. 8, and the corresponding membership function is depicted in Fig. 9.

The summary of the membership functions is presented in Table 3, including function type, linguistic variables, and parameters.

The rules of a fuzzy inference model are crucial for the effectiveness of the system, and it is necessary to define the appropriate rules and their quantity based on the problem’s nature<sup>46</sup>. The premises that guided the rules definition are detailed in the items listed below (i–vi), while Table 4 presents the nine fuzzy rules derived from these premises.

- i) If the Al(s) concentration is low, a primary factor for sweep coagulation, or if the turbidity removal is low, indicating ineffective coagulation, the sweep contribution will be very low.

- ii) The variables turbidity removal and Al(s) concentration carry equal weight.
- iii) If both turbidity removal and Al(s) concentration are at the “medium” level, the sweep contribution will be low or medium.
- iv) If one variable, either turbidity removal or Al(s) concentration is at the “medium” level and the other at the “high” level, the sweep contribution will be medium or high.
- v) If both turbidity removal and Al(s) concentration are at the “high” level, the sweep contribution will be high or very high.
- vi) If the zeta potential is neutralized, the corresponding sweep contribution will be assigned the lowest available value, as described in the previous premises.

The premises described result from the logical summation of turbidity removal and Al(s) concentration influence, both assuming equal weight for both variables, along with the influence of the zeta potential. Premise “vi” assumes that when the zeta potential is neutralized, the neutralization mechanism favors coagulation, thus leading to a lower

value of the sweep contribution in the model. When the zeta potential is strongly negative or positive, the sweep mechanism must compensate these interferences to achieve consistent coagulation performance, resulting in the higher values assigned to the sweep contribution.

### Application of the model

The output obtained from the FIS ranged from 0 to 10 after defuzzification by the centroid method. Fig. 10 presents the contour diagram of the sweep mechanism contribution, generated from the output of the proposed inference system in this study.

A well-defined zone of very low contribution is observed for dose ranges above 1.25 mg L<sup>-1</sup> and pH levels below 6.5. Intermediate contribution zones are noted at lower doses and pH levels above 6.5, extending to sweep consolidation at pH levels above 6.8 and doses above 1.75 mg L<sup>-1</sup> of Al. The zones of highest contribution, where isolated points of very high contribution are indicated in dark red, are characterized by negative or positive zeta potential, high turbidity removal, and significant formation of

Table 3 – Summary of membership functions parameters

Variable	Name	Type	Parameter
Zeta potential	Negative	Trapezoidal	[-20 -20 -10 0]
	Neutralized	Triangular	[-10 0 7]
	Positive	Trapezoidal	[0 7 25 25]
Al(s) concentration	Low	Triangular	[0 0 0.36]
	Medium	Trapezoidal	[0 0.36 1.03 1.97]
	High	Trapezoidal	[1.03 1.97 3.52 3.52]
Turbidity removal (%)	Low	Trapezoidal	[0 0 10 30]
	Medium	Trapezoidal	[10 30 60 80]
	High	Trapezoidal	[60 80 10 10]

Table 4 – Rule base of the fuzzy system relating input variables at various levels and output values

Rule	Sweep contribution
If turbidity removal is low OR insoluble Al concentration is low.	Very low
If turbidity removal is medium AND insoluble Al concentration is medium AND Zeta potential is neutralized.	Low
If turbidity removal is medium AND insoluble Al concentration is medium AND Zeta potential is negative OR positive.	Medium
If turbidity removal is medium AND insoluble Al concentration is high AND Zeta potential is neutralized.	Medium
If turbidity removal is high AND insoluble Al concentration is medium AND Zeta potential is neutralized.	Medium
If turbidity removal is medium AND insoluble Al concentration is high AND Zeta potential is negative OR positive.	High
If turbidity removal is high AND insoluble Al concentration is medium AND Zeta potential is negative OR positive.	High
If turbidity removal is high AND insoluble Al concentration is high AND Zeta potential is neutralized.	High
If turbidity removal is high AND insoluble Al concentration is high AND Zeta potential is negative OR positive.	Very high

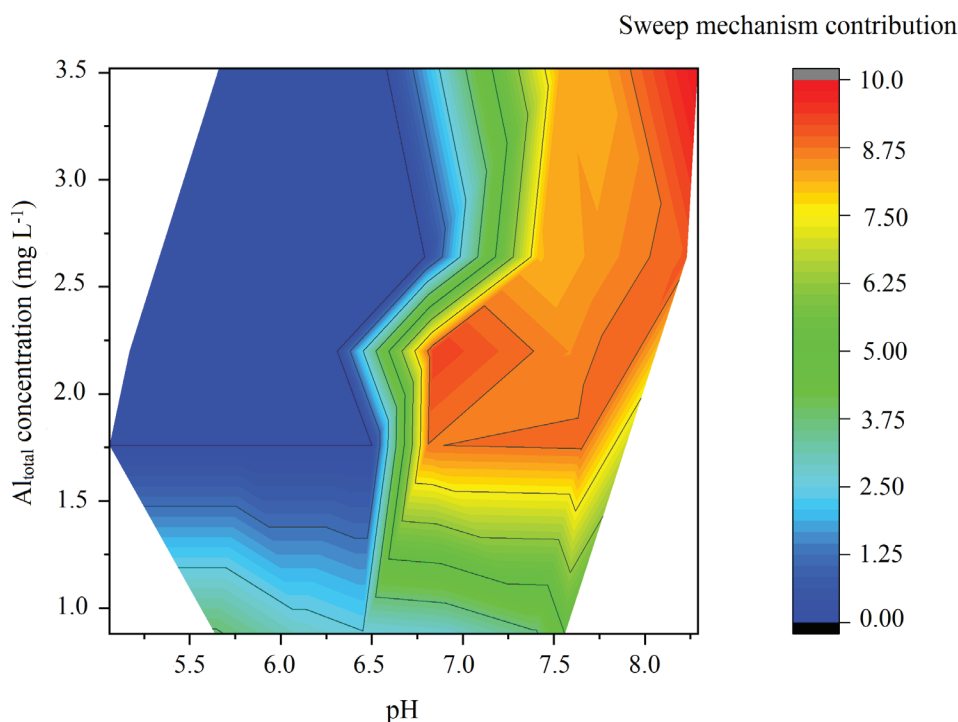


Fig. 10 – Contour diagram of the sweep mechanism contribution in the coagulation process

insoluble substances. Al(s) concentrations in the “low” range were not employed, as verified in Fig. 3, thus, the blue zone of low sweep contribution resulted from ineffective coagulation, leading to low turbidity removal.

The result, when compared to regular coagulation diagrams such as that of Arnaldos and Pagilla<sup>47</sup>, differs by providing exact values for estimating mechanism predominance rather than broad zones. This leads to more direct information that may facilitate automation commands and decision-making through simplified interpretation. Additionally, the numerical output enables a more precise identification of zones where both mechanisms, charge neutralization and sweep coagulation, occur simultaneously, by assigning specific conditions to each point instead of relying on an estimated functional division within a proposed zone. As a zone of uncertainty, this condition is addressed in the FIS through both the limits of the membership functions and the defuzzification process.

Fig. 4 illustrates that zeta potential values above 10 mV resulted in samples with low turbidity reduction. To confirm the influence zones of zeta potential, a contour diagram was created, plotting zeta potential across pH and Al dose ranges. Fig. 11 presents the distribution of zeta potential across the pH and Al dose diagram.

Interpreting Figs. 10 and 11 simultaneously, the results are consistent, with the low sweep contribution zone entirely contained within the positive zeta potential zones above 10 mV, indicating where co-

agulation does not occur. Conversely, the high contribution zone encompasses zeta potential values slightly positive ( $\sim +5$  mV) to negative values below  $-10$  mV. The highest sweep outputs are found at the extremes of this range. An expected discrete decrease was observed near zeta potential values close to 0 mV, around pH 7.25, which is indicative of the contribution of the charge neutralization mechanism, in accordance with model premise (iv). Intermediate sweep contribution zones are mainly characterized by dose ranges below  $1.5 \text{ mg L}^{-1}$  and pH levels from 6.5 to approximately 7.5, zones with intermediate turbidity removal as observed in Fig. 1.

While the diagram in Fig. 10 highlights the influence of pH on the sweep mechanism output, pH alone does not provide a reliable basis for predicting coagulation performance. This is evident in the region of medium coagulation under acidic conditions and  $\text{Al}_{\text{total}}$  concentrations below  $1.5 \text{ mg L}^{-1}$ . In contrast, one of the primary effects of pH on coagulation appears to be mediated through its influence on the zeta potential, as shown in Fig. 11. The non-coagulation zone under acidic pH was more precisely identified by high zeta potential values. This observation is supported by Nazari *et al.*<sup>48</sup>, who describe how shifts in the  $\text{H}^+/\text{OH}^-$  balance induced by pH changes disrupt the electrostatic stability of colloidal particles, thereby influencing coagulation mechanisms. These shifts can promote coagulation under conditions favorable to charge neutralization, while also delineating pathways such as sweep coagulation that are less dependent on

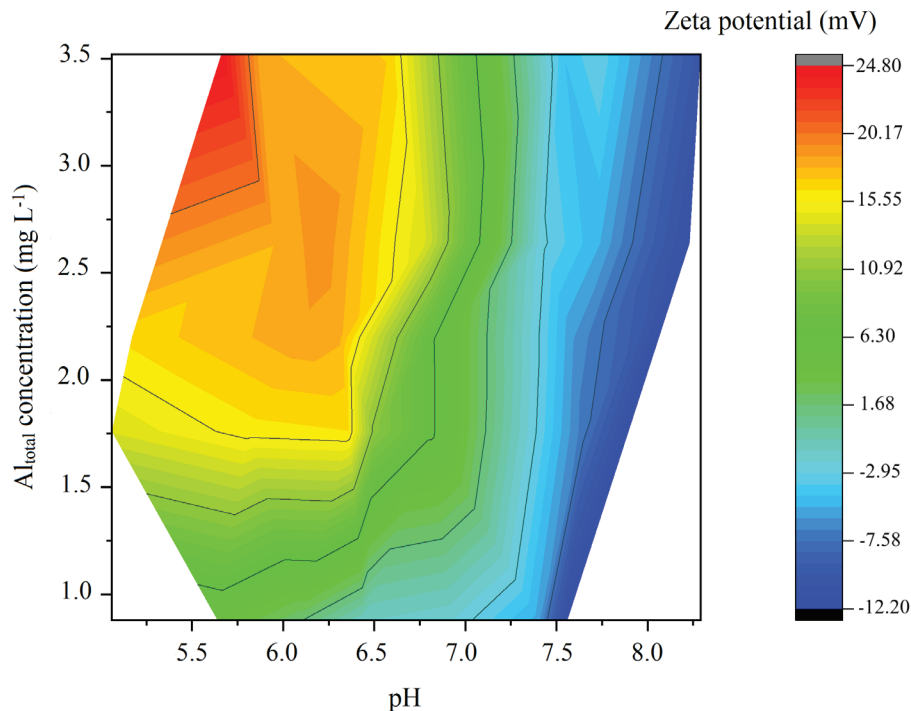


Fig. 11 – Zeta potential in relation to Al dose ( $\text{mg L}^{-1}$ ) and pH

electrostatic parameters. These results support the strategy of implicitly incorporating pH effects through the input variables zeta potential and Al(s) concentration, given the mutual interference between pH and zeta potential, and the greater informational relevance of zeta potential in characterizing the electrostatic conditions governing coagulation.

The proposed model opens opportunities to minimize the sweep mechanism contribution when the raw water is expected to be easier to treat, by maintaining the sweep coagulation output in the lower portion of the model's range. A practical application strategy for the model would involve tracking turbidity removal and comparing it with the sweep mechanism output. A zone with zero sweep output but measurable turbidity removal may indicate a region dominated by charge neutralization without floc formation, which is ideal for direct filtration and reduced sludge generation<sup>32</sup>. Alternatively, in conventional WTPs, an increase in sweep mechanism output can be desirable, particularly when driven or automated in response to a decline in turbidity removal efficiency or changes in raw water characteristics.

For the water source studied, for example, a control response, integrating continuous turbidity meters and zeta potential meters, can be adjusted to operate within the range of 1.25 to 3.75 of the mechanism, as shown in Fig. 10, with an  $\text{Al}_{\text{total}}$  dose of 1 to 1.5  $\text{mg L}^{-1}$ , and pH 5.5 to 6.5. This condition is the most economical in terms of PACl concentra-

tion. When the turbidity response indicates the need to increase the sweep mechanism, the output range from 3.75 to 6.5 would be preferred, representing  $\text{Al}_{\text{total}}$  concentrations from 1.25 to 1.75  $\text{mg L}^{-1}$  and a pH range from 6.5 to 7.5.

The control of water and wastewater processes using fuzzy models has been observed in various studies<sup>49–51</sup> and some authors highlight that linear Proportional-Integral-Derivative (PID) controllers, a highly applied control approach, have limitations when dealing with non-linear processes<sup>49,52</sup>. In a fuzzy system controlling the air supply in a wastewater treatment plant, the fuzzy model was able to integrate the practical knowledge of expert operators with simple implementation in controller design<sup>49</sup>. The authors used a trial-and-error methodology over a short period before continuous operation and evaluated the system's stability and efficiency, observing a reduction in mean squared error (MSE) with a variable set point, in contrast to a linear controller that oscillated significantly around a fixed set point. Similarly, Demirci *et al.*<sup>50</sup> describe fuzzy models for control systems in wastewater electrocoagulation treatment as robust and resistant to interference, utilizing human reasoning to control conductivity and pH. They achieved increased color and turbidity removal efficiency with the fuzzy model. Fiter *et al.*<sup>51</sup> also emphasize that fuzzy control models are easy to understand and are, therefore, better accepted by operating personnel compared to conventional models.

While knowledge-based models such as FIS are promising for process control and incorporation

into Environmental Decision Support Systems (EDSS) and automated decision-making in facilities<sup>53</sup>, concerns about computational limitations remain significant. For example, Ansari *et al.*<sup>54</sup> employed a subtractive clustering method to obtain rules and membership functions due to its lower computational effort compared to the grid partitioning method. As stated previously, Bressane *et al.*<sup>27</sup>, highlighted that ANFIS suffers from limitations related to computational expense and the clarity of decision-making, advocating for a non-hybrid data-driven FIS. The use of a model with only three input variables and nine rules, as presented in this study, is therefore important from a computational efficiency perspective.

The focus on coagulation mechanisms in this model differs from typical FIS models used in water treatment, which often concentrate on raw water quality parameters<sup>53</sup>. This model, centered on coagulation mechanisms, complements rather than replaces the capabilities of raw water quality models. Further improvements to the model could explore this synergy or identify alternatives, such as clustering specific raw water conditions to optimize the estimated contribution of the sweep mechanism for efficient treatment.

As fuzzy models inherently involve subjectivity, especially in the definition of membership functions, adapting the model to different samples may require recalibration of these functions based on the characteristics of each water sample or WTP. The limitations of the present model may be associated with the definition of membership limits, which were based on a combination of literature references and trends observed in experimental data. This is particularly relevant for the turbidity removal variable, which was defined solely based on observed trends; however, jar test results may differ from those observed in real WTPs under varying hydraulic conditions. Additionally, the characteristics of a particular raw water source may also influence zeta potential behavior in varying pairs of pH and Al dose, as well as turbidity removal, consequently the output, indicating the need for studies in different water matrices for broader validation and suggesting the need for potential model adaptations, especially regarding the membership function limits. Nevertheless, the simplicity of using three variables with three linguistic terms each facilitates easy adaptation to the specific conditions of each WTP following an initial investigation.

## Conclusion

This study developed a simplified Mamdani-type FIS to estimate the contribution of the sweep coagulation mechanism using three input variables: zeta potential, Al(s) concentration, and turbidity re-

moval. The model's structure, based on a reduced set of linguistic terms and only nine rules, was intentionally designed to offer a simplified estimation of a highly non-linear process. Beyond supporting decision-making, the FIS output enables rapid visualization of parameter interdependence and the dynamics of coagulation behavior. Its ease of adaptation to different water treatment conditions stems from its simplicity, allowing straightforward recalibration. By quantifying the sweep mechanism's contribution, the model may guide strategies to reduce reagent use and sludge generation, offering a practical and adaptable tool for real-time monitoring and potential automation in water treatment processes.

## DECLARATION OF COMPETING INTEREST

*The authors declare that they have no known competing financial interests or personal relationships that could have appeared to influence the work reported in this paper.*

## DATA AVAILABILITY

*Data will be made available on request.*

## ACKNOWLEDGMENTS

*This research was financed by the São Paulo Research Foundation, FAPESP (Grant n° 2023/12713-3), and IGTPAN – Granado Polyacrylonitrile Technology Institute.*

## References

- Garfi, M., Cadena, E., Sanchez-Ramos, D., Ferrer, I., Life cycle assessment of drinking water: Comparing conventional water treatment, reverse osmosis and mineral water in glass and plastic bottles, *J. Clean. Prod.* **137** (2016) 997. doi: <https://doi.org/10.1016/j.jclepro.2016.07.218>
- Qian, Y., Chen, Y., Hu, Y., Hanigan, D., Westerhoff, P., An, D., Formation and control of C- and N-DBPs during disinfection of filter backwash and sedimentation sludge water in drinking water treatment, *Water Res.* **194** (2021) 116964. doi: <https://doi.org/10.1016/j.watres.2021.116964>
- Jiang, J.-Q., The role of coagulation in water treatment, *Curr. Opin. Chem. Eng.* **8** (2015) 36. doi: <https://doi.org/10.1016/j.coche.2015.01.008>
- Naseem, S., Aslam, Z., Abbas, A., Sumbal, S., Ali, R., Usman, M., Synthesis and application of cobalt-based metal-organic framework for adsorption of humic acid from water, *Chem. Biochem. Eng. Q.* **36** (1) (2022) 39. doi: <https://doi.org/10.15255/CABEQ.2021.1960>
- Rezania, S., Darajeh, N., Rupani, P. F., Mojiri, A., Kamyab, H., Taghavijeloudar, M., Recent advances in the adsorption of different pollutants from wastewater using carbon-based and metal-oxide nanoparticles, *Appl. Sci.* **14** (2024) 11492. doi: <https://doi.org/10.3390/app142411492>

6. Ilyas, A., Vankelecom, I. F. J., Designing sustainable membrane-based water treatment via fouling control through membrane interface engineering and process developments, *Adv. Colloid Interface Sci.* **312** (2023) 102834. doi: <https://doi.org/10.1016/j.cis.2023.102834>
7. Surendran, D., Sakai, H., Takagi, S., Dimapilis, D. A., Tire-based microplastics: Composition, detection, and impacts of advanced oxidation processes in drinking water treatment, *Sci. Total Environ.* **972** (2025) 179114. doi: <https://doi.org/10.1016/j.scitotenv.2025.179114>
8. Venkatesan, A. K., Lee, C.-S., Gobler, C. J., Hydroxyl-radical based advanced oxidation processes can increase perfluoroalkyl substances beyond drinking water standards: Results from a pilot study, *Sci. Total Environ.* **847** (2022) 157577. doi: <https://doi.org/10.1016/j.scitotenv.2022.157577>
9. Clemente, A., Wilson, A., Oliveira, S., Menezes, I., Gois, A., Capelo-Neto, J., The role of hydraulic conditions of coagulation and flocculation on the damage of cyanobacteria, *Sci. Total Environ.* **740** (2020) 139737. doi: <https://doi.org/10.1016/j.scitotenv.2020.139737>
10. Marques, D. G., Campos, V., Estatística experimental aplicada para determinar o par ideal da dosagem de coagulante e nível de pH de coagulação para tratamento de água de abastecimento público, *Rev. Dae* **72** (2024) 44. doi: <https://doi.org/10.36659/dae.2024.004>
11. Campos, V., Domingos, J. M. F., Nolasco, M., Morais, L. C., Marques, D. G., Assessment of treatability of the Tietê River through a process of coagulation-flocculation associated with hydrodynamic cavitation and ozonation, *An. Acad. Bras. Ciênc.* **96** (2024) e20230856. doi: <https://doi.org/10.1590/0001-3765202420230856>
12. Howe, K. J., Hand, D. W., Crittenden, J. C., Trussell, R. R., Tchobanoglous, G., Princípios de tratamento de água, Cengage, São Paulo, 2016, pp. 602.
13. Wei, N., Zhang, Z., Liu, D., Wu, Y., Wang, J., Wang, Q., Coagulation behavior of polyaluminum chloride: Effects of pH and coagulant dosage, *Chin. J. Chem. Eng.* **23** (2015) 1041. doi: <https://doi.org/10.1016/j.cjche.2015.02.003>
14. Tang, S., Gao, L., Tian, A., Zhao, T., Zou, D., The coagulation behavior and removal efficiency of microplastics in drinking water treatment, *J. Water Process Eng.* **53** (2023) 103885. doi: <https://doi.org/10.1016/j.jwpe.2023.103885>
15. Allerdings, D., Förster, G., Vasyukova, E., Uhl, W., The practical influence of rapid mixing on coagulation in a full-scale water treatment plant, *Water Sci. Technol.* **71** (2015) 566. doi: <https://doi.org/10.2166/wst.2014.492>
16. Ghernaout, D., Al-Ghonamy, A. I., Naceur, M. W., Boucherit, A., Messaoudene, N. A., Aichouni, M., Mahjoubi, A. A., Elboughdiri, N. A., Controlling coagulation process: From zeta potential to streaming potential, *Am. J. Environ. Prot.* **4** (2015) 12. doi: <https://doi.org/10.11648/j.ajeps.s.2015040501.12>
17. Narges, S., Ghorban, A., Hassan, K., Mohammad, K., Prediction of the optimal dosage of coagulants in water treatment plants through developing models based on artificial neural network fuzzy inference system (ANFIS), *J. Environ. Health Sci. Eng.* **19** (2021) 1543. doi: <https://doi.org/10.1007/s40201-021-00710-0>
18. Benson, Y. A., Effect of raw water quality on coagulant dosage and optimum pH, Dissertation (Master in Civil Engineering), Technological University of Malaysia, 2006. <https://eprints.utm.my/4912/1/YannieBensonMFKA2006.pdf> (accessed 25 April 2024)
19. Silva, D. F. S., Speranza, L. G., Quartaroli, L., Moruzzi, R. B., Silva, G. H. R., Separation of microalgae cultivated in anaerobically digested black water using *Moringa oleifera* Lam seeds as coagulant, *J. Water Process Eng.* **39** (2020) 101738. doi: <https://doi.org/10.1016/j.jwpe.2020.101738>
20. Bartiko, D., Julio, M., Construção e emprego de diagramas de coagulação como ferramenta para o monitoramento contínuo da flocculação em águas de abastecimento, *Ambi-Água* **10** (2015) 71. doi: <https://doi.org/10.4136/ambi-agua.1239>
21. Martínez, M. P., Cremasco, C. P., Filho, L. R. A., Junior, S. S. B., Bednaski, A. V., Quevedo-Silva, F., Correa, C. M., Silva, D., Padgett, R. C. M. L., Fuzzy inference system to study the behavior of the green consumer facing the perception of greenwashing, *J. Clean. Prod.* **242** (2020) 116064. doi: <https://doi.org/10.1016/j.jclepro.2019.03.060>
22. Heddam, S., Bermard, A., ANFIS-based modelling for coagulant dosage in drinking water treatment plant: A case study, *Environ. Monit. Assess.* **184** (2012) 1953. doi: <https://doi.org/10.1007/s10661-011-2091-x>
23. Semiromi, B., Hassani, A., Water quality index development using fuzzy logic: A case study of the Karoon river of Iran, *Afr. J. Biotechnol.* **10** (2011) 10125. doi: <https://doi.org/10.5897/AJB11.1608>
24. Singh, N. J. A. R., Sustainable supplier selection under must-be criteria through Fuzzy inference system, *J. Clean. Prod.* **248** (2020) 119275. doi: <https://doi.org/10.1016/j.jclepro.2019.119275>
25. Tüü Szabó, B., Kóczy, L. T., A highly accurate Mamdani fuzzy inference system for tennis match predictions, *Fuzzy Optim. Decis. Mak.* **24** (2025) 99. doi: <https://doi.org/10.1007/s10700-025-09440-6>
26. Poursmaeil, H., Faramarz, M. G., Kherad, M. Z., Gheibi, M., Fathollahi-Fard, A., Behzadian, K., Tian, G., A decision support system for coagulation and flocculation processes using the adaptive neuro-fuzzy inference system, *Int. J. Environ. Sci. Technol.* **19** (2022) 10363. doi: <https://doi.org/10.1007/s13762-021-03848-4>
27. Bressane, A., Goulart, A. P. G., Melo, C. P., Gomes, I. G., Loureiro, A. I. S., Negri, R. G., Moruzzi, R., Reis, A. G., Formiga, J. K. S., Silva, G. H. R., A non-hybrid data-driven fuzzy inference system for coagulant dosage in drinking water treatment plant: Machine-learning for accurate real-time prediction, *Water* **15** (2023) 1126. doi: <https://doi.org/10.3390/w15061126>
28. Arpitha, V., Pani, A. K., Machine learning approaches for fault detection in semiconductor manufacturing process: A critical review of recent applications and future perspectives, *Chem. Biochem. Eng. Q.* **36** (1) (2022) 1. doi: <https://doi.org/10.15255/CABEQ.2021.1973>
29. Salleh, M. N. M., Talpur, N., Hussain, K., Adaptive neuro-fuzzy inference system: Overview, strengths, limitations, and solutions, in: Tan, Y., Takagi, H., Shi, Y. (Eds.), *Data Mining and Big Data*, *Lect. Notes Comput. Sci.* 10387 (2017) [Springer, Cham]. doi: [https://doi.org/10.1007/978-3-319-61845-6\\_52](https://doi.org/10.1007/978-3-319-61845-6_52)
30. Huang, C.-Y., Chen, Y.-Y., Chuang, S.-H., Hsu, Y.-S., Wu, R.-S., Ko, K.-Y., A precise dosing system based on a coagulation reaction model for water treatment, *J. Water Process Eng.* **70** (2025) 106962. doi: <https://doi.org/10.1016/j.jwpe.2025.106962>
31. Marques, D. G., Ecoeficiência do Sistema Produtor São Lourenço, *Rev. Ambientale* **13** (2021) 25. doi: <https://doi.org/10.48180/ambientale.v13i4.317>

32. Cruz, D., Pimentel, M., Russo, A., Cabral, W., Charge neutralization mechanism efficiency in water with high color turbidity ratio using aluminum sulfate and flocculation index, *Water* **12** (2020) 572.  
doi: <https://doi.org/10.3390/w12020572>
33. Xiao, F., Zhang, B., Lee, C., Effects of low temperature on aluminum(III) hydrolysis: Theoretical and experimental studies, *J. Environ. Sci.* **20** (2008) 907.  
doi: [https://doi.org/10.1016/S1001-0742\(08\)62185-3](https://doi.org/10.1016/S1001-0742(08)62185-3)
34. Shabanizadeh, H., Taghavijeloudar, M., A sustainable approach for industrial wastewater treatment using pomegranate seeds in the flocculation-coagulation process: Optimization of COD and turbidity removal by response surface methodology (RSM), *J. Water Process Eng.* **53** (2023) 103651.  
doi: <https://doi.org/10.1016/j.jwpe.2023.103651>
35. Sun, Q., Zhao, S., Yan, Y., Jia, W., Yang, W., Parameter optimization and mechanism research of enhanced coagulation treatment for Yuquan River water, *Water Supply* **20** (2020) 1072.  
doi: <https://doi.org/10.2166/ws.2020.030>
36. Sharp, E. L., Banks, J., Billica, J. A., Gertig, K. R., Application of zeta potential measurements for coagulation control: Pilot-plant experiences from UK and US waters with elevated organics, *Water Sci. Technol. Water Supply* **5** (2005) 49.  
doi: <https://doi.org/10.2166/ws.2005.0038>
37. Mroczko, D., Zimoch, I., The use of zeta potential measurement in surface water coagulation process optimization, *Proceedings* **16** (2019) 21.  
doi: <https://doi.org/10.3390/proceedings2019016021>
38. Saritha, V., Srinivas, N., Vuppala, N. V. S., Analysis and optimization of coagulation and flocculation process, *Appl. Water Sci.* **7** (2017) 451.  
doi: <https://doi.org/10.1007/s13201-014-0262-y>
39. Duan, J., Gregory, J., Coagulation by hydrolysing metal salts, *Adv. Colloid Interface Sci.* **100-102** (2003) 475.  
doi: [https://doi.org/10.1016/S0001-8686\(02\)00067-2](https://doi.org/10.1016/S0001-8686(02)00067-2)
40. Lin, J., Ika, A. R., Enhanced coagulation of low turbid water for drinking water treatment: Dosing approach on floc formation and residuals minimization, *Environ. Eng. Sci.* **36** (2019) 732.  
doi: <https://doi.org/10.1089/ees.2018.0430>
41. Yan, M., Wang, D., Yu, J., Ni, J., Edwards, M., Qu, J., Enhanced coagulation with polyaluminum chlorides: Role of pH/alkalinity and speciation, *Chemosphere* **71**(9) (2008) 1665.  
doi: <https://doi.org/10.1016/j.chemosphere.2008.01.019>
42. Trinh, T. K., Kang, L. S., Response surface methodological approach to optimize the coagulation-flocculation process in drinking water treatment, *Chem. Eng. Res. Des.* **89** (2011) 1126.  
doi: <https://doi.org/10.1016/j.cherd.2010.12.004>
43. He, W., Nan, J., Study on the impact of particle size distribution on turbidity in water, *Desalination Water Treat.* **41** (2012) 26.  
doi: <https://doi.org/10.1080/19443994.2012.664675>
44. Ng, M., Li, S., Chow, C. W. K., Drikas, M., Amal, R., Lim, M., Understanding effects of water characteristics on natural organic matter treatability by PACl and a novel PACl-chitosan coagulant, *J. Hazard. Mater.* **263** (2013) 718.  
doi: <https://doi.org/10.1016/j.jhazmat.2013.10.036>
45. Singhala, P., Shah, D. N., Patel, B., Temperature control using fuzzy logic, *Int. J. Instrum. Control Syst.* **4** (2014) 1.  
doi: <https://doi.org/10.5121/ijics.2014.4101>
46. Yazdani-Chamzini, A., Proposing a new methodology based on fuzzy logic for tunneling risk assessment, *J. Civ. Eng. Manag.* **20** (2014) 82.  
doi: <https://doi.org/10.3846/13923730.2013.843583>
47. Arnaldos, M., Pagilla, K., Effluent dissolved organic nitrogen and dissolved phosphorus removal by enhanced coagulation and microfiltration, *Water Res.* **44** (2010) 5306.  
doi: <https://doi.org/10.1016/j.watres.2010.06.066>
48. Nazari, B., Abdolalian, S., Taghavijeloudar, M., An environmentally friendly approach for industrial wastewater treatment and bio-adsorption of heavy metals using Pistacia soft shell (PSS) through flocculation-adsorption process, *Environ. Res.* **235** (2023) 116595.  
doi: <https://doi.org/10.1016/j.envres.2023.116595>
49. Baroni, P., Bertanza, G., Collivignarelli, C., Zambarda, V., Process improvement and energy saving in a full-scale wastewater treatment plant: Air supply regulation by a fuzzy logic system, *Environ. Technol.* **27** (2006) 733.  
doi: <https://doi.org/10.1080/09593332708618689>
50. Demirci, Y., Pekel, L. C., Altınten, A., Albaz, M., Application of fuzzy control on the electrocoagulation process to treat textile wastewater, *Environ. Technol.* **36** (2015) 3243.  
doi: <https://doi.org/10.1080/09593330.2015.1058423>
51. Fiter, M., Güell, D., Comas, J., Colprim, J., Poch, M., Rodríguez-Roda, I., Energy saving in a wastewater treatment process: An application of fuzzy logic control, *Environ. Technol.* **26** (2005) 1263.  
doi: <https://doi.org/10.1080/09593332608618596>
52. Emori, E. Y., Ravagnani, M. A. S. S., Costa, C. B. B., An advanced control strategy for the evaporation section of an integrated first- and second-generation ethanol sugarcane biorefinery, *Chem. Biochem. Eng. Q.* **37** (1) (2023) 17.  
doi: <https://doi.org/10.15255/CABEQ.2022.2048>
53. Godo-Pla, L., Rodríguez, J. J., Suquet, J., Emiliano, P., Valero, F., Poch, M., Monclús, H., Control of primary disinfection in a drinking water treatment plant based on a fuzzy inference system, *Process Saf. Environ. Prot.* **145** (2021) 63.  
doi: <https://doi.org/10.1016/j.psep.2020.07.037>
54. Ansari, M., Othman, F., El-Shafie, A., Optimized fuzzy inference system to enhance prediction accuracy for influent characteristics of a sewage treatment plant, *Sci. Total Environ.* **722** (2020) 137878.  
doi: <https://doi.org/10.1016/j.scitotenv.2020.137878>